Landau levels and band bending in few-layer epitaxial graphene

Hongki Min,[1,2,*] S. Adam,[1] Young Jae Song,[1,2] Joseph A. Stroscio,[1] M. D. Stiles,[1] and A. H. MacDonald[3]

[1]*Center for Nanoscale Science and Technology, National Institute of Standards and Technology, Gaithersburg, Maryland 20899-6202, USA*

[2]*Maryland NanoCenter, University of Maryland, College Park, Maryland 20742, USA*

[3]*Department of Physics, University of Texas at Austin, Austin, Texas 78712, USA*

The carrier density distributions in few-layer-graphene systems grown on the carbon face of silicon carbide can be altered by the presence of a scanning tunneling microscope (STM) tip used to probe top-layer electronic properties, and by a perpendicular magnetic field which induces well-defined Landau levels. Hartree approximation calculations in the perpendicular field case show that charge tends to rearrange between the layers so that the filling factors of most layers are pinned at integer values. We use our analysis to provide insight into the role of buried layers in recent few-layer-graphene STM studies and discuss the limitations of our model.

I. INTRODUCTION

Progress in the preparation and isolation of highly ordered graphene sheets over the past few years[1,2] has led to an explosion of interest in the properties of these two-dimensional electron systems which are remarkably simple, yet rich in interesting mechanical and electronic properties. One type of graphene system[2] that is potentially suitable for applications is prepared by thermal decomposition of silicon carbide (SiC). The unique feature of these *epitaxial graphene* systems is that they tend to grow not as single layers but as few-layer-graphene (FLG) systems. The layers tend to be electrically isolated to a reasonable degree[3–7] because of partially controlled relative rotations.[8,9] FLG systems on SiC can be grown as large area films that are extremely highly ordered, at least locally, and doped by charge transfer from a carbon buffer layer, which is a nongraphitic carbon layer between the SiC and the graphene layers.

This paper addresses the distribution of charge carriers across the FLG system. Recent measurements of Landau-level spectra[10,11] and angle-resolved photoemission[12] for FLG systems grown on the carbon face of SiC show characteristics of decoupled monolayer graphene rather than coupled graphene multilayers. This behavior is likely due to the relative rotations between the layers. Our work is motivated in part by an interest in understanding the confusing[13] transport properties of these systems, which must be strongly dependent on carrier charge distribution across the weakly coupled layers. Our immediate motivation, however, is provided by recent[11,14] scanning tunneling microscopy (STM) Landau-level spectroscopy studies of FLG in the presence of an external magnetic field. Traces of the Landau-level positions can be extracted from such spectra as is illustrated in Fig. 1. Although STM directly probes electronic properties in the top layer of a FLG system, there is evidence that top-layer properties can be altered, sometimes qualitatively, by correlations with electrons in submerged layers.

If the density in the top layer were fixed, the Fermi level would be pinned to one of the Landau-level energies except at the discrete field strengths which yield integer filling factors when the Fermi level is in between Landau levels. In practice, experiment shows the opposite behavior. The Landau levels

tend to be pinned away from the Fermi energy, an effect that is particularly striking in the field range between 8 T and 10 T. At higher fields, the Landau levels split through valley and spin splitting so that even in the field range near 12 T, the split Landau levels avoid the Fermi energy.

The most dramatic effect seen in these experiments is splitting within spin- and valley-split $N = 1$ peaks in the density of states (DOS) as they pass through the Fermi level.[14] This peculiar, fractionally filled Landau level gives evidence for a correlated-electron state that is stable when the $N = 1$ Landau level of the top layer is half filled.

While the precise nature of this state remains mysterious, its formation might depend only on correlations among top-layer electrons; however, if one of the submerged layers is also partially filled under the same tip-biasing and field conditions, then this fractionally filled Landau level could depend essentially on correlations between electrons in different layers. Since half filling does not favor the formation of especially stable states in an isolated layer, the latter possibility appears likely. In the strong-magnetic-field quantum Hall regime with fully formed Landau levels only weakly broadened by disorder, correlations are strongest when Landau levels are partially filled. One goal of the model developed in this paper attempts to provide a basis for estimating which layers contain partially filled Landau levels as the magnetic field strength varies.

Our paper is organized as follows. In Sec. II, we explain our model for carrier distribution in a few-layer-graphene system in which the buffer layer acts as a reservoir for carriers. We assume that the growth-dependent buffer-layer properties determine the position of the Fermi energy relative to the Dirac point of the bottom graphene layer. Electron-electron interactions are included only at the Hartree level. At zero magnetic field carriers reside mainly in the layers closest to the buffer and the density of states in the top layer is small. When a perpendicular magnetic field is applied, the Fermi level tends to be pinned near one of the filling factors ($\nu = \pm 2, \pm 6, \pm 10, \ldots$) at which the integer quantum Hall effect occurs in a graphene layer, implying that charge must be transferred between layers as a function of field. In Sec. III, we discuss how an STM tip can be included in such a model. When an STM tip is introduced to study the electronic properties
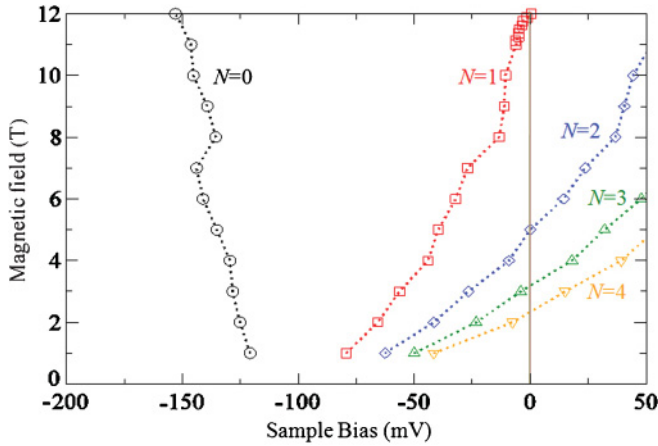
FIG. 1. (Color online) Landau-level peak positions of epitaxial graphene on C-face SiC as a function of magnetic field obtained from the STM measurements in Ref. 14. The position of each Landau level is averaged over spin and valley split dI/dV peaks when these can be separately resolved (Ref. 15). dI/dV peak positions at finite tip-sample bias can be influenced by tip-sample band bending and by redistributions of charge in the FLG system as explained in detail below.

of the top layer, its carrier density tends to be altered with a sign and magnitude that is strongly dependent on the tip work function. The STM studies in Refs. 11,14 show that the top layer is n type for the tip used in those experiments, so that carrier densities peak not only near the buffer layer but also near the top layer. In Sec. IV, we use this basic theoretical picture to develop a theory of STM Landau-level spectroscopy in FLG, comparing where possible with STM data. We find that as the sample-tip bias and the magnetic field are varied, charge tends to rearrange to achieve integer filling factors in as many of the FLG layers as possible. In Sec. V, we conclude with a brief summary and some suggestions for future experimental and theoretical work.

II. FEW-LAYER-GRAPHENE MODEL

We estimate carrier charge distribution in a FLG system grown on carbon-face SiC substrates using the model summarized schematically in Fig. 2. Earlier work considered the charge distribution on mono- and bilayer graphene[16] and for multilayer graphene[17] in the continuum limit, both in the absence of a magnetic field, our main interest. In Fig. 2, the graphene layers are labeled by integer numbers starting from label 1 for the layer closest to the buffer layer to M for the top layer. (The buffer layer between the SiC and the graphene layers, which acts as a reservoir for carriers, was omitted for simplicity.) In equilibrium all layers share the same chemical potential μ. The Dirac point in layer i is shifted by its local electric potential u_i. The energy spectrum of each layer is that of monolayer graphene with the Dirac point shifted by u_i. It follows that the charge density in layer i, σ_i, satisfies

$$\sigma_i = \frac{\mathrm{sgn}(\mu - u_i)}{\pi} \left(\frac{\mu - u_i}{\hbar v} \right)^2 . \tag{1}$$
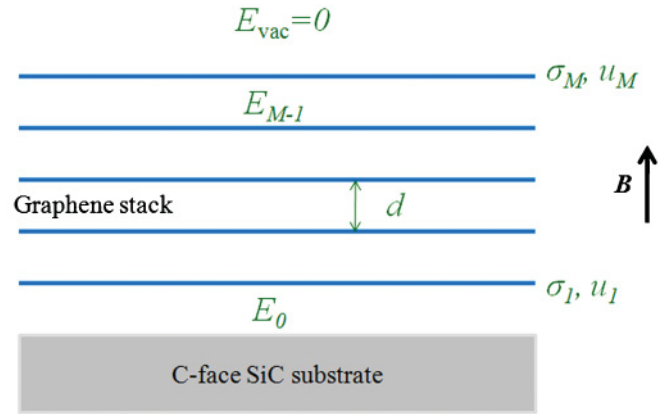

FIG. 2. (Color online) Schematic illustration of a few-layer-graphene system without an STM tip. The buffer layer between the SiC and the graphene layers was omitted for simplicity.

The potential energy u_i is in turn evaluated from the charge densities using the Poisson equation which implies that the electric field E_i between layer i and layer $i + 1$ satisfies

$$\epsilon \left(E_i - E_{i-1} \right) = 4\pi (-e)\sigma_i . \tag{2}$$

The dielectric constant ϵ in Eq. (2) accounts for the polarizability between graphene sheets. Here we choose $\epsilon = 1$; we have found that changing the value of ϵ does not qualitatively alter the main results of this paper.

Since the electric field in the vacuum above the top (Mth) layer E_{vac} must vanish in the absence of an STM tip, the electric fields between all graphene sheets are readily evaluated iteratively given the charge densities σ_i. Starting from layer 1 and adding a contribution due to the electric field between a layer and the layer above gives

$$u_{i+1} = u_i + ed E_i, \tag{3}$$

where $d = 0.335$ nm is the interlayer separation between graphene layers. Our neglect of interaction effects beyond electrostatics is supported in the zero magnetic field limit by recent Green's function screened Coulomb (GW) many-body calculations[18] by Profumo *et al*. As we discuss below, exchange and correlation effects are likely to be more important in large magnetic fields.

We model the role of the buffer layer by assuming that its equilibration with the bottom graphene layer fixes the value of $\mu - u_1$. It is known that the carrier density of the graphene system is sensitive to the microstructure of the disordered buffer layer, and hence to FLG growth conditions. For a given sample, some carriers remain after the bonding between the buffer layer and the SiC substrate is established. Energy in the system is lowered as these electrons are transferred to the π bands of the first graphene layer. u_1 is determined by a balance between the chemical driving force for the transfer and the band and electrostatic energy cost of adding electrons to the graphene. In assuming that u_1 is independent of field, as we do below, we are taking advantage of the fact that the Landau-level separation at the Fermi energy of the first graphene sheet is small compared to $\mu - u_1$. In modeling STM data on a particular sample, imperfect knowledge of the most appropriate value for $\mu - u_1$ is an important

source of uncertainty that limits predictive power. For the calculations described below we choose $\mu - u_1 = 360$ meV, an estimate that is motivated by spectroscopic measurements[19] in multilayer graphene grown on the C face of the SiC substrate. In the rest of this paper we choose our zero of energy so that $u_1 = 0$.

To explain how band and electrostatic energies combine to determine carrier distributions, we first consider double-layer graphene with a chemical potential $\mu > 0$. From the Poisson equation with $E_{\text{vac}} = 0$, the electric field between layers, E, satisfies $\epsilon E = 4\pi e \sigma_2$. The potential energy of the top layer is $u_2 = eEd$. It follows that

$$\sigma_1 = \frac{1}{\pi}\left(\frac{\mu}{\hbar v}\right)^2, \tag{4}$$

$$\sigma_2 = \frac{\text{sgn}(\mu - u_2)}{\pi}\left(\frac{\mu - u_2}{\hbar v}\right)^2$$

$$= \frac{\text{sgn}(\mu - u_2)}{\pi}\left(\frac{\mu}{\hbar v}\right)^2 f(\beta),$$

where

$$f(\beta) = (\sqrt{\beta^2 + 2\beta} - \beta)^2 \tag{5}$$

and $\beta = \epsilon(\hbar v)^2/(8e^2 d\mu)$ is a unitless quantity which controls the energy balance of charge moving between layers. Here v is the π-band velocity at the Dirac point which is proportional to the intralayer hopping energy γ_0. For $\mu = 360$ meV, $\epsilon = 1$, and $\gamma_0 = 3$ eV, $\beta \approx 0.29$ and $f(\beta) \approx 0.28$; thus the top layer has 28% of the bottom-layer charge.

For multilayers with more than two layers, the distribution follows from a simple numerical calculation. The layer charge density is calculated by integrating the Landau-level density of states weighted by the Fermi factor for the appropriate chemical potential. Then from the resulting layer densities, layer potentials are calculated using the Poisson equation in Eq. (2). This process is repeated until a self-consistency is reached.

The charge distribution for a decoupled 6-layer graphene stack at $B = 0$ T and $B = 10$ T calculated with the same

parameters used in the double-layer graphene is shown in Fig. 3. For $B = 0$ T, layers above the bottom layer have in total 32% of the bottom-layer charge and this ratio is almost independent of the number of layers. As the magnetic field is turned on, the charge distribution is altered due to the formation of Landau levels, particularly in the low-density layers with a Fermi level near the Dirac point. Because a Landau level appears precisely at the Dirac point in a graphene sheet, a magnetic field causes a peak in the density of states to appear at the same energy at which the density of states vanishes in the absence of a magnetic field. This feature of graphene physics strengthens magnetoelectric effects associated with Landau-level quantization.

III. STM TIP MODEL

Figure 4 shows a schematic illustration of a FLG system with an STM tip. We model an STM tip as an additional layer

FIG. 4. (Color online) Upper panel shows schematic illustration of a few-layer-graphene system with an STM tip. The buffer layer between the SiC and the graphene layers was omitted for simplicity. Lower panel is the energy level diagram for this system.
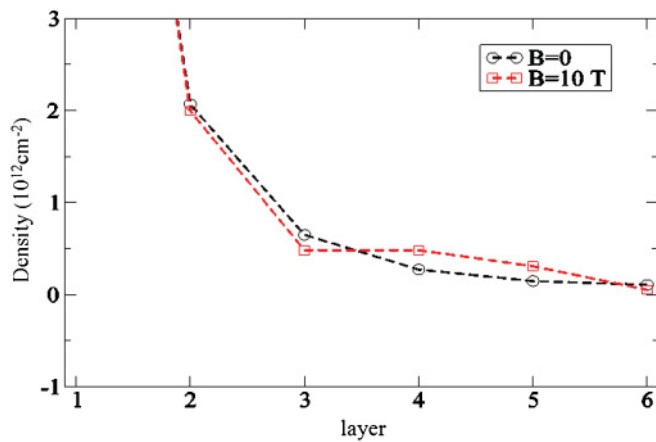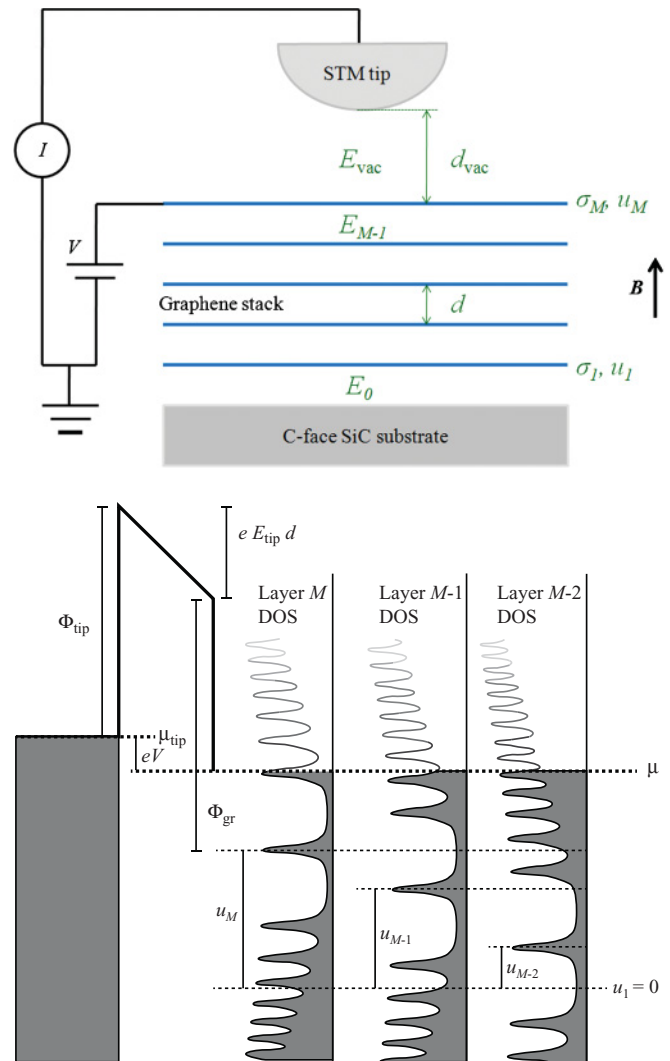

FIG. 3. (Color online) Charge density vs layer index for a 6-layer FLG system at $B = 0$ T and $B = 10$ T. Here chemical potential $\mu = 360$ meV and temperature $T = 30$ K were used.

which acts as a top gate electrode. The distance between the tip and graphene surface is taken as $d_{\text{vac}} = 1$ nm.[20]

Experimentally, it is found that the graphene work function, i.e., the energy to take an electron from the Fermi energy to vacuum, depends on the charge on the surface layer. However, it is also found that the energy to take a graphene electron from the Dirac point to vacuum does not change as a function of the charge density.[21] We denote the latter as Φ_{gr}. In general, the work function of the tip (Φ_{tip}) and the graphene layer [$\Phi_{\text{gr}} - (\mu - u_M)$] are different. This difference in work functions, $\Phi_{\text{gr}} - (\mu - u_M) - \Phi_{\text{tip}} \equiv \Phi - (\mu - u_M)$, leads to charge transfer between the surfaces when they are electrically connected and induces an electric field between the surface and tip. As seen in the bottom panel of Fig. 4, the electric field satisfies

$$\mu + eV = \mu^{\text{tip}} = u_M + eE_{\text{vac}}d_{\text{vac}} + \Phi \qquad (6)$$

as a voltage V is applied between tip and sample.

In STM spectroscopy a new tunneling transport channel opens up, giving rise to a dI/dV peak whenever the chemical potential of the STM tip is aligned with one of the top-layer Landau levels. The experimental dI/dV peaks therefore identify the tip-sample bias voltages at which the following resonant tunneling conditions are satisfied:

$$\mu + eV = u_M + \varepsilon_N(B), \qquad (7)$$

where $\varepsilon_N(B) = \text{sgn}(N)\sqrt{2|N|e\hbar v^2 B/c}$ is the graphene-sheet Landau-level energy. To illustrate the effect of the tip, in Fig. 5 we calculate the charge distribution of each layer at $B = 10$ T for $\Phi = +0.4$ eV, 0 eV, and -0.4 eV when the tip-sample bias V is zero.

For $\Phi = 0$ eV and $V = 0$ V, the FLG charge distribution is identical to the distribution without an STM tip at $B = 10$ T shown in Fig. 3. For nonzero Φ, however, an electric field between the tip and sample surface is induced and distorts the layer charge distribution even at zero tip-sample bias.
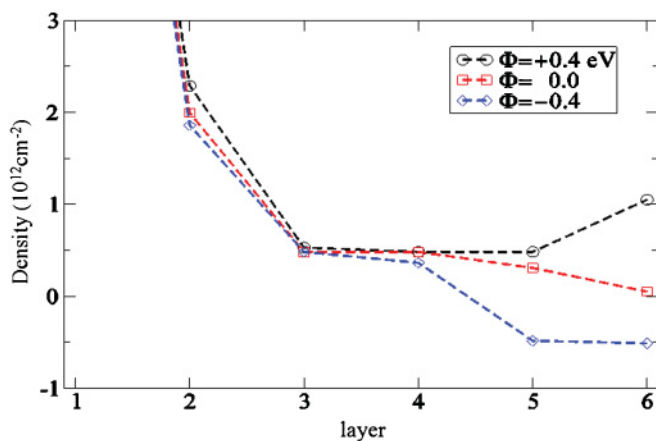

FIG. 5. (Color online) Charge density in the layers of a six-layer stack at $B = 10$ T for $\Phi = +0.4$ eV, 0 eV, and -0.4 eV when the tip-sample bias is zero. These curves were obtained using $\mu = 360$ meV and $T = 30$ K. By construction, electrons have a positive carrier density, while holes have negative density (see text for details).
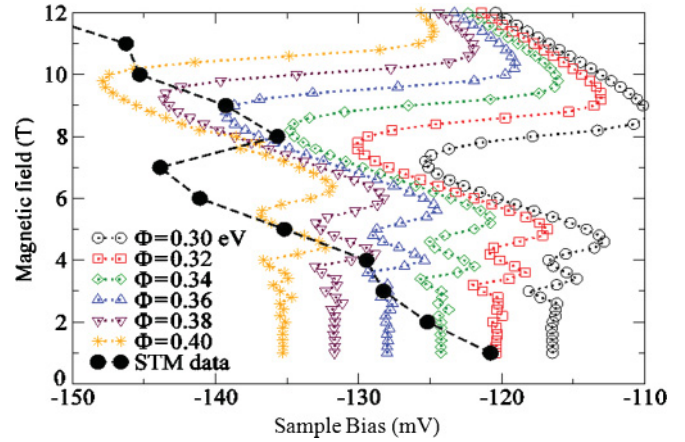

FIG. 6. (Color online) The field dependence of the $N = 0$ Dirac-point Landau level for different work-function parameters Φ (Ref. 15). Here $\mu = 360$ meV and $T = 30$ K were used.

IV. FLG LANDAU-LEVEL TUNNELING SPECTROSCOPY

At weak fields, u_M and E_{vac} are approximately constant so that the spacing in electronvolts between dI/dV peaks matches the energetic separation between top-layer Landau levels. The spectroscopy data can therefore be used to measure the Dirac velocity parameter which characterizes the energy scale of the graphene layer's Dirac cones. In the strong-field limit, however, the density of states in each graphene layer is altered, and this in turn alters the densities at which equilibria are established between adjacent layers. It follows that both u_M and E_{vac} depend on field. One goal of our calculations is to estimate the magnitude and character of this effect.

To illustrate this effect we first examine the field dependence of the $N = 0$ Dirac-point Landau-level feature, plotted in Fig. 6. Since $\varepsilon_{N=0}(B) \equiv 0$, the field dependence of this spectral feature is due entirely to the field dependence of charge distributions in the FLG system. The calculations in Fig. 6 were carried out at a finite temperature $T = 30$ K, in part to crudely model the Landau-level smearing influence of disorder. At weak fields the $N = 0$ dI/dV peak's position is independent of field as expected. The position of these peaks is primarily dependent on the model's work-function parameter Φ.

As illustrated in Fig. 6, the position of the experimental peak at $eV \approx -135$ meV and at $B = 5$ T is reproduced approximately by setting $\mu = 360$ meV, which leads to $u_M \approx 225$ meV and $\Phi \approx 400$ meV. The slow downward drift in the weak-field $N = 0$ Dirac point peak with increasing magnetic field is not reproduced by our calculation, and could be due to an increase in the strength of exchange and correlation effects in FLG with magnetic field. The strong variations in peak positions with field that begin at around 6 T are the quantizing-magnetic-field effects on which we will focus in the remainder of this paper.

The influence of Landau quantization on dI/dV spectra is illustrated in more detail in Fig. 7, which shows the prediction of the theoretical model for $\Phi = 400$ meV and $\mu = 360$ meV at $T = 30$ K.

When the Landau-level energies in a particular layer are far away from the Fermi energy, the layer filling factor $\nu_i = 2\pi\ell^2\sigma_i$, where $\ell = \sqrt{\hbar c/eB}$ is pinned at one of the
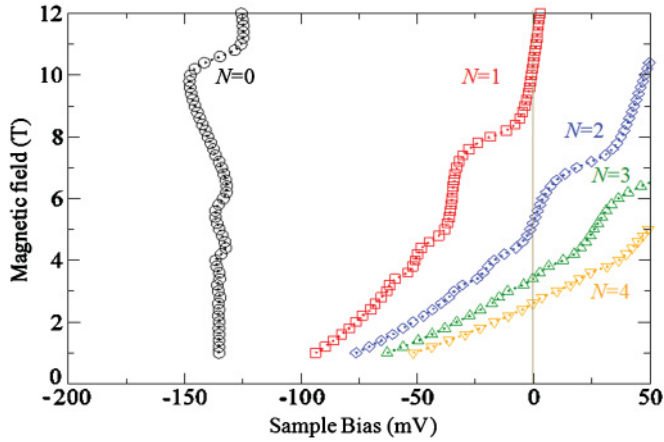
FIG. 7. (Color online) Theoretical prediction of top-layer Landau-level peak positions as a function of magnetic field for $\Phi = 400$ meV and $\mu = 360$ meV at $T = 30$ K.

full-Landau-level filling factor values: $\nu_i = \pm 2, \pm 6, \pm 10, \cdots$. For a fixed filling factor the carrier density in a layer increases with field and its Landau level energies therefore increase due to electrostatic repulsion. The increase in density must be achieved by charge transfer from other layers. When a Landau level in a layer is close to the Fermi level, the density in that layer will tend to decrease as its Landau level empties with increasing field. This is the source of charge transferred to other layers. This behavior contrasts with that of an isolated system with fixed charge density in which integer filling factors occur only at isolated field values and successive Landau-level energies are pinned to the Fermi level.

We refer to layers which have partially filled Landau levels as *active* and to layers which have full Landau levels as *inactive*. Since the total filling factor is a smooth function of field, at least one layer must be active at generic field values. Strong interlayer correlations are likely when two or more layers are active. It would be surprising if interlayer correlation effects were not important, given the relationship between the important length scales in the problem. At 10 T, the total graphene-layer thickness $Md \approx 2$ nm is typically much less than the average separation of electrons within one layer $1/\sqrt{\sigma_i} \approx 10$ nm as well as the magnetic length $\ell = \sqrt{\hbar c/eB} \approx 8.1$ nm. Such correlations could give rise to a state with spontaneous interlayer coherence[14] among other possibilities. As shown below, our model calculations provide estimates of the field ranges at which two or more layers become active.

For the parameters of Fig. 7 the model predicts that the top layer is active between $B = 5$ T and $B = 7$ T. In this field range the $N = 2$ Landau level is pinned to the Fermi level and the filling factor varies between $\nu = 10$ and $\nu = 6$.[22] The top layer is then briefly inactive before becoming active again above 8 T when the $N = 1$ Landau level is pinned to the Fermi level. In inactive field ranges, the density in the top layer is proportional to magnetic field and the energies of all levels in that layer increase. In the active regions, the density tends to decrease and the rate at which energy levels increase with field for $N > 0$ is suppressed by the decrease in density. This is only a tendency, however, since the electrostatic energy in the
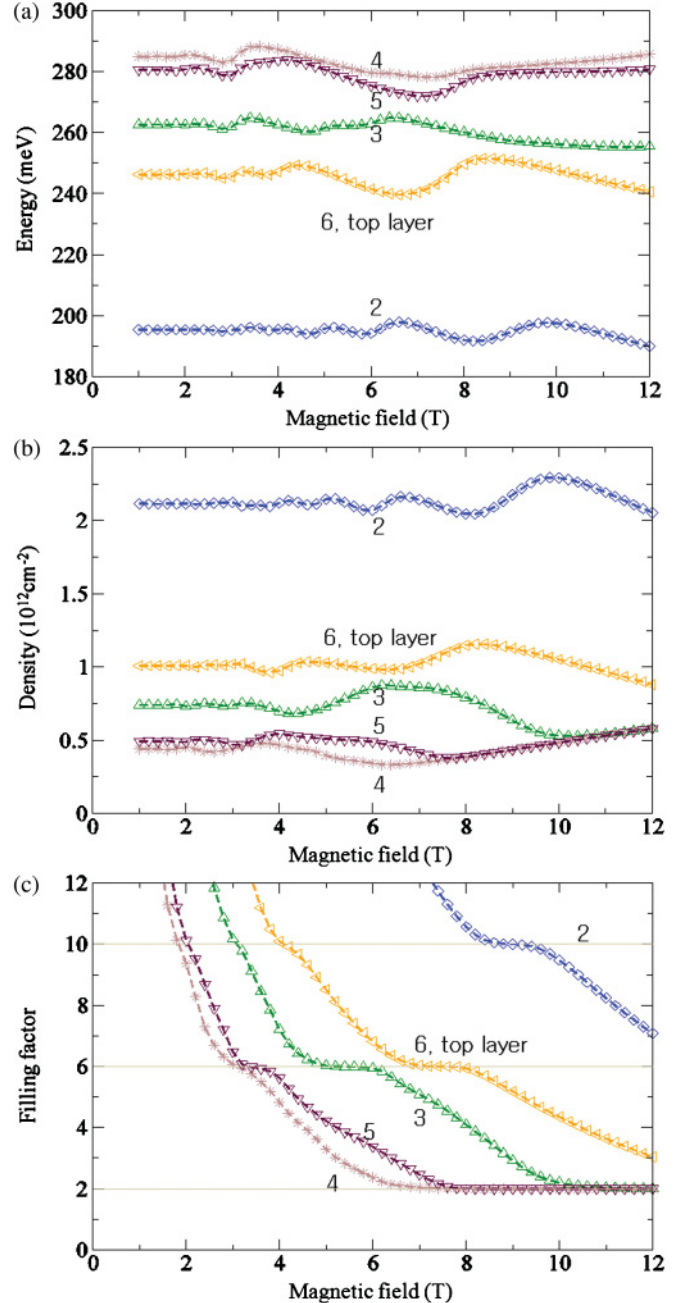

FIG. 8. (Color online) Electrostatic energy, density, and filling factor of each layer as a function of magnetic field for $\Phi = 400$ meV, $\mu = 360$ meV, and $T = 30$ K at zero tip-sample bias voltage. The filling factor of the bottom layer (not shown) exceeds $\nu = 12$ over the field range considered. Numbers indicate layer numbers, with 6 being the topmost layer.

top layer depends on the densities at all layers. The evolution of the STM spectrum also depends on the evolution of charge density in the submerged layers that are not directly probed by the STM. Note that the distribution of charge among the FLG layers also depends somewhat on the tip-sample bias voltage. Figure 8 shows the electrostatic energy, density, and filling factor of each layer as a function of magnetic field at zero bias voltage. These results are consistent with the preceding discussion.
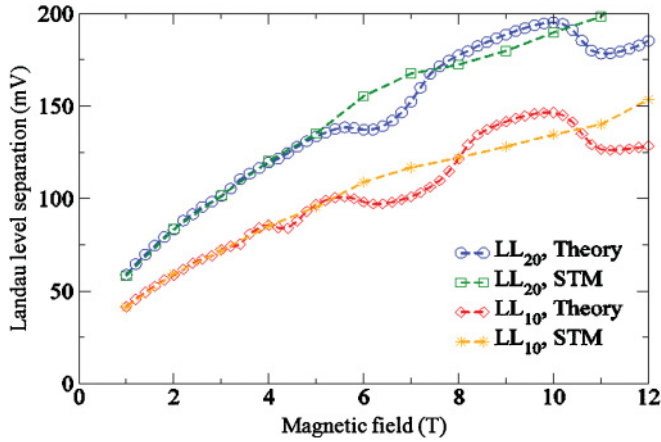
FIG. 9. (Color online) Landau-level separations between $N = 0$ and the $N = 1$ ($N = 2$), denoted as LL_{10} (LL_{20}) for theoretical calculations and STM measurements (Ref. 15). For the theoretical calculations, $\Phi = 400$ meV and $\mu = 360$ meV at $T = 30$ K were used.
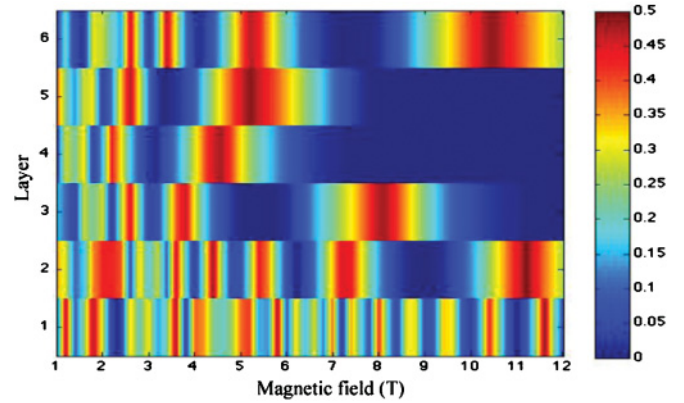

FIG. 10. (Color online) Filling factor modulus ν_i^{mod} as a function of magnetic field for $\Phi = 400$ meV and $\mu = 360$ meV at $T = 30$ K, where $\nu_i^{\mathrm{mod}} = |(\nu/4 \ \mathrm{mod} \ 1) - 1/2|$. Note that $\nu_i^{\mathrm{mod}} = 0$ for $\nu_i = \pm 2, \pm 6, \pm 10, \cdots$, while $\nu_i^{\mathrm{mod}} = 1/2$ for $\nu_i = 0, \pm 4, \pm 8, \cdots$. The points were evaluated at zero bias voltage.

V. DISCUSSION AND CONCLUSIONS

Our theoretical model does not account for exchange and correlation effects, which can alter the energy change associated with adding electrons to empty (or partially filled) Landau levels and the energy change associated with removing electrons from full (or partially full) Landau levels. Systematic discrepancies between present theory and experiment likely signal these neglected interaction effects. These discrepancies include the low field variation of the zeroth-Landau-level energy (Fig. 6) and the pinning of the first Landau level away from the Fermi energy rather than at it (Fig. 1).

In Fig. 9, for example, we compare experimental and theoretical energy separations between $N = 0$ and the $N = 1, 2 \ dI/dV$ features as a function of magnetic field strength. Even at the Hartree level there are additions to the $\sqrt{B}$ band energy contribution due to changes in electrostatic energies with tip-sample bias voltages indicating overestimation of the electrostatic tip-gating effects.

We note that the filling-factor-dependent features in the field dependence of the Landau-level energies [Fig. 8(c)] are weaker in experiment than in this Hartree theory. We believe that these differences mainly reflect exchange and correlation energies which mitigate electrostatic effects. The presence of strong correlation effects in this field range is apparent in the experimental interaction-induced Landau-level splittings which have been suppressed in Fig. 9 by averaging over all experimental features identified with $N = 0$ and $N = 1$.

The approximately linear reduction with field (at weak fields) of the bias voltage at which the $N = 0$ peak is observed (see Fig. 6) is completely absent in theory and unexplained at present.

In addition to effects associated with exchange and correlation within a layer, we expect that interlayer correlations play an essential role when more than one layer is active, at least when the magnetic field is strong and Landau levels are well developed. In Fig. 10 we plot the field dependence of the partial filling factor (per layer and spin) of the active Landau level: $\nu_i^{\mathrm{mod}} \equiv |(\nu/4 \ \mathrm{mod} \ 1) - 1/2|$, which we refer to as the modular filling factor. ν_i^{mod} is defined so that it vanishes when a Landau level is either completely filled or completely empty, namely at total filling factors $\nu_i = \pm 2, \pm 6, \pm 10, \cdots$. Note that the layer is inactive when $\nu_i^{\mathrm{mod}} = 0$, and most active when $\nu_i^{\mathrm{mod}} = 0.5$. Around $B = 11$ T, we see that the top (6th) layer and the 2nd layer have filling factors close to half-filled filling factors, $\nu_6 = 4$ and $\nu_2 = 8$, respectively (in this field range the intervening layers all have total Landau-level filling factor $\nu = 2$). This is precisely the field range in which a gap appears to open in the top layer $N = 1$ tunneling density of states in STM studies.[14] The gap could therefore be due to correlations between $N = 1$ electrons in the top layer and $N = 2$ electrons in layer 2. The participation of electrons in another layer could explain the appearance of a gap at a partial filling factor which is not known to support large gaps in a single-layer system. One possible state that is consistent with experiments is one in which coherence is spontaneously[23] established between layers 2 and 6. Around $B = 5$ T and below, the top layer and 5th layers become active, but due to the smaller field magnitude, strong correlation effects are more easily suppressed by disorder.

The analysis presented in this paper highlights both advantages and disadvantages of few-layer-graphene systems for physics studies. Because the electronic degrees of freedom in all layers can play an active role, particularly at strong magnetic fields, the physics is extremely rich. On the other hand, the same property makes it more challenging to uniquely interpret observations using surface physics probes, like STM, which are directly sensitive mainly to top-layer properties.

*hmin@umd.edu; Current address: Condensed Matter Theory Center, Department of Physics, University of Maryland, College Park, Maryland 20742, USA.

[1] For recent reviews, see T. Ando, Phys. Soc. Jpn. **74**, 777 (2005); A. K. Geim and K. S. Novoselov, Nature Mater. **6**, 183 (2007); A. H. Castro Neto, F. Guinea, N. M. R. Peres, K. S. Novoselov, and A. K. Geim, Rev. Mod. Phys. **81**, 109 (2009); S. Das Sarma, S. Adam, E. H. Hwang, and E. Rossi, e-print arXiv:1003.4731, Rev. Mod. Phys. (to be published 2011).

[2] P. N. First, W. A. de Heer, T. Seyller, C. Berger, J. A. Stroscio, and Jeong-Sun Moon, MRS Bull. **35**, 296 (2010).

[3] J. M. B. Lopes dos Santos, N. M. R. Peres, and A. H. Castro Neto, Phys. Rev. Lett. **99**, 256802 (2007).

[4] S. Shallcross, S. Sharma, E. Kandelaki, and O. A. Pankratov, Phys. Rev. B **81**, 165105 (2010).

[5] G. Trambly de Laissardiére, D. Mayou, and L. Magaud, Nano Lett. **10**, 804 (2010).

[6] E. J. Mele, Phys. Rev. B **81**, 161405(R) (2010).

[7] R. Bistritzer and A. H. MacDonald, Phys. Rev. B **81**, 245412 (2010).

[8] Z. Y. Rong and P. Kuiper, Phys. Rev. B **48**, 17427 (1993).

[9] J. Hass, F. Varchon, J. E. Millan-Otoya, M. Sprinkle, N. Sharma, W. A. de Heer, C. Berger, P. N. First, L. Magaud, and E. H. Conrad, Phys. Rev. Lett. **100**, 125504 (2008).

[10] M. L. Sadowski, G. Martinez, M. Potemski, C. Berger, and W. A. de Heer, Solid State Commun. **143**, 123 (2007).

[11] D. L. Miller, K. D. Kubista, G. M. Rutter, M. Ruan, W. A. de Heer, P. N. First, and J. A. Stroscio, Science **324**, 924 (2009).

[12] M. Sprinkle, D. Siegel, Y. Hu, J. Hicks, A. Tejeda, A. Taleb Ibrahimi, P. Le Fèvre, F. Bertran, S. Vizzini, H. Enriquez, S. Chiang, P. Soukiassian, C. Berger, W. A. de Heer, A. Lanzara, and E. H. Conrad, Phys. Rev. Lett. **103**, 226803 (2009).

[13] P. Darancet, N. Wipf, C. Berger, W. A. de Heer, and Didier Mayou, Phys. Rev. Lett. **101**, 116806 (2008); W. A. de Heer, C. Berger, X. Wu, M. Sprinkle, Y. Hu, M. Ruan, J. A. Stroscio, P. N. First, R. Haddon, B. Piot, C. Faugeras, M. Potemski, and J-S. Moon, J. Phys. D **43**, 374007 (2010).

[14] Y. J. Song, A. F. Otte, Y. Kuk, Y. Hu, D. B. Torrance, P. N. First, W. A. de Heer, H. Min, S. Adam, M. D. Stiles, A. H. MacDonald, and J. A. Stroscio, Nature (London) **467**, 185 (2010).

[15] Experimental peak energy positions were determined by fitting a Lorentzian function to the measured Landau level peaks. The positions are averaged over typically 50 spectra with one standard deviation statistical uncertainties typically less than 1 mV, which is smaller than the plotted symbol size.

[16] S. Kopylov, A. Tzalenchuk, S. Kubatkin, and V. I. Falko, Appl. Phys. Lett. **97**, 112109 (2010).

[17] S. S. Datta, D. R. Strachan, E. J. Mele, and A. T. Charlie Johnson, Nano Lett. **9**, 7 (2009).

[18] R. E. V. Profumo, M. Polini, R. Asgari, R. Fazio, and A. H. MacDonald, Phys. Rev. B **82**, 085443 (2010).

[19] D. Sun, C. Divin, C. Berger, W. A. de Heer, P. N. First, and T. B. Norris, Phys. Rev. Lett. **104**, 136802 (2010).

[20] J. A. Stroscio and W. J. Kaiser, *Scanning Tunneling Microscopy, Methods of Experimental Physics* (Academic Press, Boston, 1993).

[21] Y.-J. Yu, Y. Zhao, S. Ryu, L. E. Brus, K. S. Kim, and P. Kim, Nano Lett. **9**, 3430 (2009).

[22] Note however that the temperature we use here to simulate disorder broadening effects is much larger than measured Landau level widths. We were unable to obtain convergence at substantially lower temperatures. In some cases, a lack of convergence in Hartree-level calculations may signal that interlayer correlations play an essential role in the physics.

[23] J. P. Eisenstein and A. H. MacDonald, Nature (London) **432**, 691 (2004).